THE JOURNAL OF PHYSICAL CHEMISTRY B

 VOLUME 106, NUMBER 35, SEPTEMBER 5, 2002

LETTERS

Electronic Structure of the P_{700} Special Pair from High-Frequency Electron Paramagnetic Resonance Spectroscopy

Oleg G. Poluektov,*,† Lisa M. Utschig,† Sandra L. Schlesselman,† K. V. Lakshmi,‡ Gary W. Brudvig,‡ Gerd Kothe,§ and Marion C. Thurnauer*,†

Chemistry Division, Argonne National Laboratory, 9700 South Cass Avenue, Argonne, Illinois 60439, Department of Chemistry, Yale University, P.O. Box 208107 New Haven, Connecticut 06520-8107, and Department of Physical Chemistry, University of Freiburg, Albertstrasse 21, D-79104 Freiburg, Germany

Received: June 21, 2002; In Final Form: July 23, 2002

Enhanced spectral resolution of high-frequency electron paramagnetic resonance (EPR) spectroscopy allows for detailed g-tensor analysis of the active paramagnetic pigments in photosynthetic reaction centers. This analysis has been made for the cation radical and triplet state of the primary donor in photosystem I (P_{700}) compared to the same species from chlorophyll *a* (Chl*a*) in vitro. The data prove that the electronic structures of the primary donor cation and triplet state are very different from those of monomeric Chl*a*. The g-value anisotropy of $P_{700}^{+\bullet}$ is smaller, and the g_z component considerably deviates from that of Chl$a^{+\bullet}$. The triplet state of P_{700} is also different from Chla^{T}. In the present study, this difference is resolved because of the high g-value resolution of the high-frequency EPR and characterized by the switching of the directions of the *X* and *Y* g-tensor axes with respect to the zero-field axes. These results can be explained either by a delocalized electronic character of the $P_{700}^{+\bullet}$ and P_{700}^{T} states or by a heteromeric model of the primary donor in photosystem I.

1. Introduction

Photosynthetic energy conversion performed by bacteria, plants, or algae occurs in membrane protein complexes known as reaction center proteins (RCs). The primary light reactions involve electron transfer from the photoexcited primary electron donor (P) to a series of electron acceptors resulting in charge separation across the membrane.[1,2] On the basis of magnetic resonance data,[3] it was proposed that the primary donors for different RCs consist of a closely positioned pair of specific chlorophyll (Chl) molecules, that is, a pair of bacteriochlorophyll *a* (Bchl*a*) molecules (P_{850}) in *Rhodobacter sphaeroides* and a pair of chlorophyll *a* (Chl*a*) molecules (P_{700}) in photosystem I (PS I) of green plants. Recently, X-ray diffraction analysis[4,5] confirmed the presence of the structural Chl pairs in the photosynthetic proteins. The recently reported 2.5 Å resolution structure of the photosystem I RC protein reveals that P_{700} is a Chl*a*/Chl*a*′ "heterodimer", in which Chl*a*′ is the $C13^2$ epimer of Chl*a*.[5] X-ray analysis, however, cannot provide information on the electronic coupling or electronic structure of the chlorophyll dimers. Importantly, the electronic structure of the primary donors determines their redox properties. The oxidation potential of the primary donors in photosynthetic RCs is considerably higher than those of the respective monomeric chlorophyll molecules, Bchl*a* and Chl*a* in vitro. This is believed to be due to the pairing of the chlorophyll molecules, which, in

* To whom correspondence should be addressed. Fax: (630) 252-9289. E-mail addresses: Oleg@anl.gov and Mariont@anl.gov.
† Argonne National Laboratory.
‡ Yale University.
§ University of Freiburg.

10.1021/jp021465+ CCC: $22.00
Published on Web 08/14/2002

turn, facilitates an efficient charge separation in the RC proteins. Thus, the electronic structures of the primary donors, particularly in their active states (excited P*, triplet P^T, and oxidized $P^{+\bullet}$), have been the focus of much research. In particular, the excited triplet and oxidized states have been studied extensively with electron paramagnetic resonance (EPR) spectroscopy.

In the case of the bacterial RCs from *Rhodobacter sphaeroides*, it has been established that the primary donors are "real" dimers, that is, excitation in P* and densities of unpaired electrons in $P^{+\bullet}$ and P^T states are delocalized over both chlorophyll molecules, though a slight asymmetry (2:1) is observed.[3,6−8] As for the primary donor in PS I, data confirming either monomeric or dimeric electronic structures are very controversial. The initial interpretation of EPR data on $P_{700}^{+\bullet}$ suggested that this species is a dimer.[3] However later results and interpretations claimed both monomeric or dimeric electronic structures.[9−17] Thus, the question is still not resolved. A detailed chronological review of this controversy concerning the electronic structure of P_{700} is presented in a recent article devoted to this problem.[18] The main contradiction is that from the magnetic resonance studies (EPR, ENDOR, ESEEM) a pure monomeric[9,11] or very asymmetric (>6:1)[11,17,18] spin-density distribution in $P_{700}^{+\bullet}$ is found while FTIR and optical data reveal a dimer structure with a symmetric distribution of the spin density.[12] For the triplet state P_{700}^T, there is evidence from EPR experiments that at room-temperature triplet excitation is delocalized over the two halves of a Chl*a* dimer[16] but localized on one of the Chl*a* molecules at low temperature.[14,15] This conclusion is based on the experimental fact that the zero-field parameters of P_{700}^T compared to those of Chla^T are the same at low temperatures and slightly smaller at room temperature.

High-frequency EPR spectroscopy can offer additional independent support in favor of the monomeric or the dimeric model. Providing high resolution of the g-tensor, high-frequency EPR spectroscopy can detect small changes in the magnetic resonance parameters of $P_{700}^{+\bullet}$ and P_{700}^T compared to Chl$a^{+\bullet}$ and Chla^T. Because the g-tensor is a fingerprint of the electronic structure of a paramagnetic center, comparison of the g-values of the paramagnetic states of the primary donor with those of monomeric Chl*a* can shed light on the electron spin-density distribution in the primary donor.

The g-tensors of $P_{700}^{+\bullet}$ and Chl$a^{+\bullet}$ were measured at high EPR frequency by a number of groups.[19−23] These data were collected under different experimental conditions (temperatures, magnetic fields, microwave cavities, microwave powers, modulation amplitudes) and with different g-value calibration procedures. The latter, in combination with line shape distortions due to fast-passage effects,[22,23] is the main source of errors in the g-value measurements. This leads to the large scatter of the experimental g-values that can be found in the literature. While the reported anisotropy of the g-tensors, or relative measurements of the canonical g-values within one spectrum, is very similar, the absolute g-values are often outside the claimed experimental errors, making comparison difficult. To minimize the error and make the absolute g-values comparable, we have conducted the measurements of the magnetic resonance parameters of $P_{700}^{+\bullet}$, Chl$a^{+\bullet}$, P_{700}^T, and Chla^T under the same experimental conditions, using the same calibration procedure and g-value reference marker.

In this communication, we present high-frequency EPR data that can be interpreted as delocalization of the $P_{700}^{+\bullet}$ and P_{700}^T states in PS I. The g-value anisotropy of $P_{700}^{+\bullet}$ is smaller than that of the so-called chlorophyll Z (Chl(z)) cation radical in photosystem II (PS II) and Chl$a^{+\bullet}$ in methylene chloride. Moreover, the g_z component of the g-tensor of $P_{700}^{+\bullet}$ considerably deviates from that of Chl$a^{+\bullet}$ and Chl(z)$^{+\bullet}$ and from the free electron value. This can be explained by effective averaging of the g-value in the dimer of chlorophyll molecules in $P_{700}^{+\bullet}$. The magnetic resonance parameters of P_{700} triplet state are also different from those of the chlorophyll *a* triplet. This difference is resolved because of the high g-value resolution of high-frequency EPR and characterized by the switching of the *X* and *Y* g-tensor axes directions with respect to the zero-field axes. Thus, in contrast with previous studies, the triplet state of P_{700} deviates considerably from Chla^T. To our knowledge, these are the first measurements of the magnetic resonance parameters of the P_{700}^T and Chla^T by high-frequency EPR spectroscopy.

2. Experimental Section

Deuterated Chl*a* was extracted from 99% deuterated cells of *Scenedesmus obliquus*. References for the deuteration and extraction procedures can be found in ref 22. Solutions of 10^{-3} M Chl*a* in methylene chloride or toluene were prepared. To prevent aggregation 10 vol % of pyridine was added to the toluene solution. Oxidation of Chl*a* was carried out with a stoichiometric amount of iodine in a glovebox filled with nitrogen gas. Deuterated PS I and PS II complexes were isolated from deuterated whole *Synechococcus lividus* cells using the procedure described elsewhere.[23] The sample was loaded onto a DEAE column in the absence of $MgSO_4$. PS II was eluted with a 1-L gradient of 0−50 mM $MgSO_4$-containing buffer, and PS I was collected by elution with 0.5-L of 100 mM $MgSO_4$-containing buffer (50 mM MES−NaOH (pH 6.0), 20 mM $CaCl_2$, 5 mM $MgCl_2$, 25% (w/v) glycerol, and 0.03% β-dodecyl maltoside). The PS II and PS I fractions were analyzed by UV−visible spectroscopy and SDS-PAGE. For the preparation of the triplet state P_{700}^T, the PS I complex was treated with dithionite (pH 10) and preilluminated at 75 K, which leads to the reduction of iron−sulfur centers and phylloquinone. Preparation of the deuterated Mn-depleted PS II samples and generation of the Chl(z)$^{+\bullet}$/Car$^{+\bullet}$ signal were carried out as described in ref 23.

High-frequency EPR spectra were recorded at D-band (130 GHz/4.6 T) with a continuous wave/pulsed EPR spectrometer described previously.[23] A cylindrical single-mode cavity TE_{011} was used, having slits on the cylindrical side of the cavity to allow for optical excitation and field modulation. Precision measurement of the high magnetic field (with an accuracy of 10^{-6}) in a superconducting magnet is restricted by its stability and homogeneity characteristics. As a rule, the magnetic field is homogeneous in a very small confined region (~10 mm), which is completely occupied by the EPR probe. This makes it problematic to use a magnetometer to measure the magnetic field at the sample during the EPR experiment. To overcome this problem, a reference sample, which is placed in the cavity together with the sample under study, is used. We used Mn^{2+} impurities in a commercially available powder of MgO as a g-value marker. The powder as a point reference sample was glued on the surface of the plunger between the sample tube and the walls of the cylinder. The plunger with g-marker was oriented in such way that the B_1 field on the reference sample was perpendicular to the main magnetic field. In this geometry, the intensity of the reference Mn^{2+} signal is maximum. Only six hyperfine lines ($I = {}^5/_2$) with a line width of ~1 G from the $m_s = \pm{}^1/_2$ transition of Mn^{2+} are observed at high magnetic field. Hyperfine splitting between the lines allows the use of the Mn^{2+} signal as both g- and field-sweep markers at the same time. The g-value of the Mn^{2+} was calibrated using an aqueous

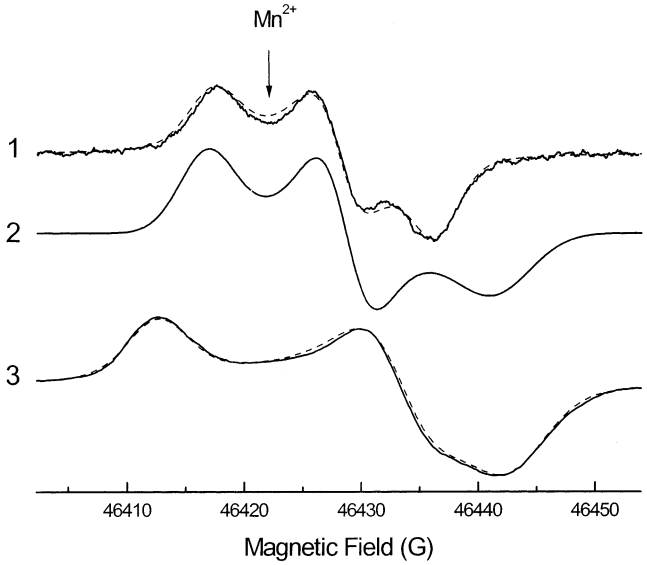

Figure 1. D-band EPR spectra recorded at 70 K: (1) cation radical of primary donor P_{700} in deuterated photosystem I (dashed line is a simulation); (2) simulated spectra of the deuterated chlorophyll *a* cation radical obtained from the deconvolution of overlapping chlorophyll/carotenoid signals in photosystem II (for details see ref 25); (3) cation radical of primary donor P_{865} in deuterated bacterial reaction center protein from *Rhodobacter sphaeroides* (dashed line is a simulation). Arrow indicates position of one of the Mn^{2+} hyperfine lines, which were used as field markers. Spectra of the radicals with Mn^{2+} marker were recorded in a separate experiment (not shown here).

solution of Fremi salt. This radical has narrow EPR lines and its magnetic resonance parameters were measured with high accuracy by X-band EPR: $g_{iso} = 2.00550 \pm 0.00004$; $A_{iso} = 13.091 \pm 0.004$ G.[24] The effective g-value (the middle between third and forth hyperfine components) and effective hyperfine splitting (the splitting between third and forth hyperfine components) for Mn^{2+} were determined as $g_{eff} = 2.00122 \pm 0.00004$, $A_{eff} = 86.7 \pm 0.1$ G.[25] Note that the difference between the effective and intrinsic g-values at the given magnetic field is due to the second-order terms.

Samples were illuminated in the cavity of the EPR spectrometer. Light excitation was achieved with an optical parametric oscillator (Opotek) pumped by a Nd:YAG laser (Quantel). The output of the laser was coupled to a fiber optic to deliver light to the cavity (1 mJ/pulse). The excitation wavelength was 550 nm. The sample temperature was regulated by an Oxford temperature controller (ITC 503) coupled to an Oxford continuous-flow cryostat (CF 1200). The simulation program SIMFONIA from Bruker Instruments Inc. was used for simulations of the spectra.

Spectra of the triplet states of Chl*a* and P_{700} were recorded using the time-resolved electron spin−echo technique. Two microwave pulses followed a short 10 ns laser pulse after a fixed delay time. The triplet spectra were recorded by monitoring electron spin−echo intensity as a function of the magnetic field. Variation of the delay after laser flash (DAF) time allows one to follow the dynamics of the triplet sublevel electron populations.

3. Results and Discussion

$P_{700}^{+\bullet}$ and Chl$a^{+\bullet}$ Cation Radicals. EPR spectra of the $P_{700}^{+\bullet}$ and $Chl(z)^{+\bullet}$ cation radicals are shown in Figure 1. The spectrum of $Chl(z)^{+\bullet}$ is a simulated spectrum, which was obtained from the deconvolution of the Chl(z)/carotenoid (Car) cation radical signal recorded in PS II as described in ref 23. Note that the chemical structure of Chl(z) is identical to the structure of Chl*a*.[26] We were not able to record a well-resolved spectrum of Chl*a* cation radical in methylene chloride or toluene solutions because the line widths of the canonical components of the Chl$a^{+\bullet}$ are always broader in vitro than those observed in the protein environment. This effect was previously reported for protonated Chl$a^{+\bullet}$[22] and explained by the g-strain effect. The strain is caused by heterogeneity in either chlorophyll−solvent interactions or conformation structures of chlorophyll molecules. This observation demonstrates that the protein environment has a high homogeneity and a spread in the conformational structures is very small compared to the glassy state of the isotropic solvents. The same conclusion on the homogeneity of the bacterial RC proteins has been made from the analysis of the line width of the primary donor and chlorophyll triplet states.[15]

The $Chl(z)^{+\bullet}/Car^{+\bullet}$ spectrum was recorded with a Mn^{2+} marker signal to calibrate absolute values of the $Chl(z)^{+\bullet}$ g-tensor. The relative g-values or g-value anisotropy (the difference between $g_x - g_z$ and $g_y - g_z$ values) is in agreement with the data obtained for deuterated Chl$a^{+\bullet}$ in methylene chloride at 327 GHz EPR frequency.[22] Relative g-value measurements are more accurate than absolute measurements, because the accuracy of the absolute g-value measurements is usually restricted by the line width, ΔH (peak position can be determined with the accuracy of $0.1\Delta H$), whereas relative measurements depend on the simulation of the spectral line shape and thus are more precise. The similar anisotropy of the g-tensors obtained for $Chl(z)^{+\bullet}$ and Chl$a^{+\bullet}$ (see Table 1) proves that the deconvolution procedure is correct. This also indicates that the protein environment is very similar to the low molecular weight glassy environment and the electronic structure of the chlorophyll *a* in the protein is not disturbed.

Recording the $P_{700}^{+\bullet}$ and Chl$a^{+\bullet}$ cation radicals under similar experimental conditions and with the same Mn^{2+} reference signal allows us to make a comparative analysis of their g-values. The results presented in Table 1 and Figure 1 show that the anisotropy of the $P_{700}^{+\bullet}$ signal is considerably smaller than that of Chl$a^{+\bullet}$. The most important observation is that the g_z component of $P_{700}^{+\bullet}$ has the largest shift compared to the g_z component of Chl$a^{+\bullet}$. This shift, 19×10^{-5} is considerably greater than the accuracy of the absolute g-tensor measurements, which we estimate to be 5×10^{-5}. The value of the g_z shift and the fact that the g_z component has the largest perturbation for $P_{700}^{+\bullet}$ cannot be explained in the framework of a monomeric Chl$a^{+\bullet}$ for the primary donor cation. Indeed, the classical Stone's theory of the g-values[27] predicts shifts of the radical g-values due to the interaction with the environment. The shifts are caused by the unpaired electron spin density redistribution and changes in the energy of the occupied and unoccupied orbitals. According to Stone's theory, the shift in the g_z component, the component for which the value is closest to the free electron value of 2.0023, is a second-order effect (order of magnitude smaller) compared to the shifts of the g_x and g_y components. On the contrary, the experimentally observed shifts of the g_x and g_y peaks of $P_{700}^{+\bullet}$ compared to Chl$a^{+\bullet}$ are smaller than the shift of g_z. Thus, the observed $P_{700}^{+\bullet}$ spectrum cannot be explained simply by the interaction of the protein environment with a monomeric chlorophyll *a* species.

On the other hand, the delocalization of the spin density of the unpaired electron between the two chlorophyll molecules of the "special pair" can account for the observed shift of g_z and decrease in the anisotropy of the g-tensor in $P_{700}^{+\bullet}$ compared to Chl$a^{+\bullet}$. In this case, the g-values are effectively averaged

TABLE 1: Magnetic Resonance Parameters of $P_{700}^{+\bullet}$, Chl$a^{+\bullet}$, P_{700}^{T}, and Chla^{T} Obtained by Simulation of the Experimental Spectra Presented in Figures 1 and 2

sample	g_x	g_y	g_z	$g_x - g_z$	$g_x - g_y$	$g_y - g_z$	D (10^{-4} cm^{-1})	E (10^{-4} cm^{-1})
$P_{700}^{+\bullet}$[a]	2.00329	2.00282	2.00246	83	47	36		
Chl$a^{+\bullet}$[a,b]	2.00332	2.00280	2.00225	107	52	55		
P_{700}^{T}[c]	2.00369	2.00323	2.00252	117	46	71	280 ± 1	39.0 ± 0.2
Chla^{T}[c]	2.00344	2.00382	2.00265	79	−38	117	284 ± 1	41.3 ± 0.2

[a] The notation of *X*, *Y*, and *Z* g-tensor axes is a standard one and counts from the lower to higher magnetic field, respectively. Error in the absolute measurements of the g-values is $\pm 5 \times 10^{-5}$. The relative measurements of Δg within one radical are more accurate, $\pm 2 \times 10^{-5}$, because they are based on the simulation of the line shape of the spectrum. [b] The data were collected for Chl(z) cation radical, which has a chemical structure identical to Chl*a*.[26] [c] The notation of *X*, *Y*, and *Z* axes is standard for triplet sublevels with positive *D*: the sublevel energy in the zero-field approximation is increasing from *Z* to *X*. The g-tensor is measured as a middle point between respective zero-field components. Error in the absolute and relative g-values is $\pm 9 \times 10^{-5}$. It is larger than that for the cation radicals because of the broad line width and wide spread of the spectra.

out between the two molecules, leading to a decrease of the total g-value anisotropy. The shift of the g_z component may be the same order of magnitude or even higher than that for the g_x and g_y components. A quantitative analysis of the delocalization based on these g-tensor measurements is not currently feasible. The mutual geometry of the Chl*a* molecules in the dimer and the orientation of the g-tensor in the molecular frame of the chlorophyll are required for a quantitative analysis. While the former is available from recent X-ray diffraction analysis,[5] the orientation of the g_x and g_y components in the plane of the chlorophyll molecule is not known precisely.[22] Moreover, even a small rearrangement of the spin density on the dimer halves in $P_{700}^{+\bullet}$ as compared with Chl$a^{+\bullet}$[10] or mixing of the ground state with a closely lying excited state, proposed in ref 28 will considerably influence a quantitative analysis.

A dimer structure of $P_{700}^{+\bullet}$ can qualitatively explain the observed substantial deviation of the g-tensor axis from the molecular axis of the chlorophyll molecule.[29,30] The main discrepancy is a deviation of the g_z axis of ~30° from the normal to the molecular plane,[29,30] which is in contradiction with the g-tensor theory of Stone.[27] According to the theory, it should coincide with the normal to the plane of planar π radicals. This deviation logically follows from the structure of the two chlorophyll species assigned to P_{700}[5] if we assume a delocalization of the spin density over the two molecules. The chlorin planes of the two chlorophyll species are parallel, are 3.6 Å apart from each other, and partially overlap.[5] The two planes are shifted in such a way that the central Mg^{2+} ions are separated by 6.3 Å. For this geometry, the deviation of the g_z axis from the molecular normal follows from symmetry considerations. It is interesting to note that this geometry suggests delocalization of the unpaired electron spin density over the two chlorophyll species. As the separation between the chlorophylls is smaller, the overlap is larger[5] and, as a consequence, $\pi-\pi$ interactions are assumed to be stronger compared to those in the primary donor in bacterial reaction centers ($Mg^{2+}-Mg^{2+}$ separation is 7.6 Å), where the unpaired electron spin density is believed to be delocalized.

Another suggestion for the delocalization of the spin density in $P_{700}^{+\bullet}$ comes from analysis of the spectral line width. The g_z component of $P_{700}^{+\bullet}$ has a surprisingly small line width. From the simulation of the $P_{700}^{+\bullet}$ spectrum, the Gaussian line width of the g_z component is $\Delta H_Z = 3.8$ G, the same as that for g_y, $\Delta H_Y = 3.8$ G, and smaller than that for g_x, $\Delta H_X = 4.2$ G. On the other hand, the Chl$a^{+\bullet}$ line width, ΔH_Z, should be the largest because it is determined by the unresolved ^{14}N hyperfine couplings. These hyperfine couplings are anisotropic and have the largest value along the *Z* axis, which is perpendicular to the chlorin plane.[29,30] This is indeed the case for Bchl$a^{+\bullet}$ (data are not shown) and Chl$a^{+\bullet}$,[22] for which ΔH_Z is 1.5−2 times greater than ΔH_X and ΔH_Y. The simulated Chl$a^{+\bullet}$ spectrum

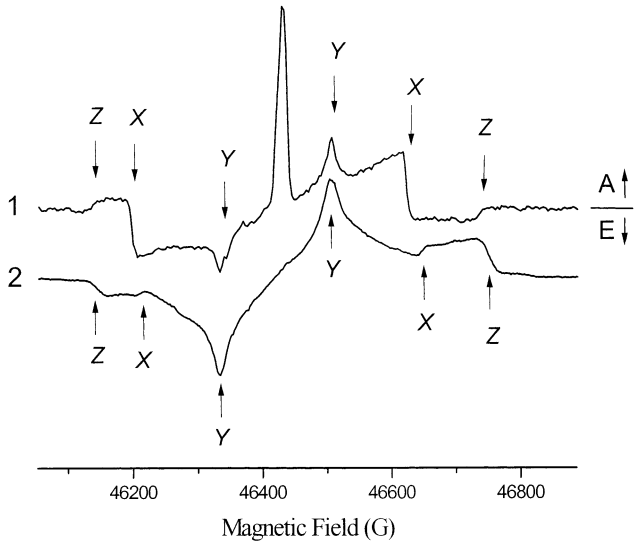

Figure 2. Time-resolved D-band polarized EPR spectra of the triplet states recorded by pulsed EPR technique: (1) triplet state of primary donor P_{700} in deuterated photosystem I (strong absorption peak in the middle of the spectra is due to the cation radical of P_{700}); (2) triplet state of the deuterated chlorophyll *a* in toluene/pyridine (90:10) solvent. The microwave pulse (p) sequence used in the experiment was $t_{p1}-\tau-t_{p2} = 40$ ns−300 ns−60 ns; DAF (delay after flash) time equals 3 μs; optical excitation wavelength $\lambda = 550$ nm; temperature equals 75 K. *X*, *Y*, and *Z* in combination with arrows indicate positions of the turning points in the spectra, which correspond to the main orientation of the zero-field tensor. A and E show absorption and emission parts of the spectra, respectively.

presented in Figure 1 displays the same trend: $\Delta H_Z = 6.4$ G, $\Delta H_Y = 4.0$ G, and $\Delta H_X = 4.7$ G. An averaging of the magnetic resonance parameters between the two halves of a P_{700} dimer could be responsible for the relatively small line width of the g_z component in $P_{700}^{+\bullet}$. It is interesting that a similar trend is observed in the primary donor $P_{865}^{+\bullet}$ of the bacterial reaction center protein, in which a delocalization of the electron spin density is assumed. However, the difference in the line width between the canonical components is smaller: $\Delta H_Z = 6.1$ G, $\Delta H_Y = 5.6$ G, and $\Delta H_X = 5.0$ G.

P_{700}^{T} and Chla^{T} Triplet State. The high-frequency EPR spectra of the P_{700} and Chl*a* triplet states are shown in Figure 2. The positions of the canonical components corresponding to the main orientation of the zero-field tensor are marked by arrows. The splitting between these arrows is defined by the zero-field parameters *D* and *E*: 2*D* for *Z* axis, $D - 3E$ for *Y* axis, and $D + 3E$ for *X* axis in the standard notation of the triplet sublevels in the low-field approximation.[15] These parameters are summarized in Table 1 and are in agreement with previously reported data.[13−16] The spectra of P_{700} and Chl*a* triplet

states exhibit electron spin polarization (ESP). The so-called "T_0" ESP of the P_{700}^T has been explained by the radical pair mechanism of the triplet formation and the EAEAEA pattern of the Chl*a*^{T} by spin−orbit coupling.[15]

Recording the triplet-state EPR spectra at high magnetic field allows direct measurement of the projection of the g-tensor component on the direction of the zero-field axis. Analysis of the data, presented in the Table 1, demonstrates a striking effect. The ordering of the g_x and g_y components is switched between P_{700}^T and Chl*a*^{T}. This effect is clearly seen although, because of the large spread of the triplet spectrum and relatively broad line width of the canonical components, the absolute error in the g-value measurement is $\sim 9 \times 10^{-5}$ higher than that for the cation radicals.

The effect can only be explained by the different orientation of the zero-field axis with respect to the g-tensor main axis in P_{700}^T compared to Chl*a*^{T}. This means that, while the values of the zero-field parameters of these two triplet states are very close, the distributions of the spin densities are very different. The conclusion that the spin density is localized on one of the two chlorophylls in the triplet state of P_{700} primary donor was based on the similarities of the magnetic parameters.[14,15] Thus, in contrast to what was shown before, the present study indicates that the triplet state of P_{700} deviates considerably from Chl*a*^{T}. To our knowledge, this is the first measurement of the magnetic resonance parameters of the P_{700}^T and Chl*a*^{T} by high-frequency EPR spectroscopy.

A reasonable explanation for the switching between the *X* and *Y* axes may be the delocalization of the electron spin density over the two chlorophyll species assigned to the primary donor. Unfortunately, speculation on the geometry and spin delocalization for such a dimer is not possible on the basis of these experimental data for the same reason that it was not possible for the g-tensors of the cation radical. The orientations of the g-tensor axes and zero-field axes in the molecular frame are missing. Moreover, a possible contribution of charge-transfer character to the triplet state of the primary donor[15] will complicate an analysis based on simple averaging of the g- and zero-field axes. To answer these questions, an extended theoretical study of these systems is needed.

It should be noted that rotation of the triplet−triplet and Q_Y transition moments of P_{700} with respect to the zero-field *X* and *Y* axes of P_{700}^T compared to those of the respective Chl*a* states in organic glasses has been observed by linear-dichroic absorbance-detected magnetic resonance (LD-ADMR) measurements.[31] The authors ascribe this observation to the effect of the environment.

A similar effect, switching of the *X* and *Y* zero-field axes with respect to the molecular axes, has been observed previously in transient X-band EPR studies of Chl*a* dissolved in a liquid crystal.[32] The spin-polarized triplet spectra showed a peculiar dependence on the excitation wavelength of the laser, indicating the existence of monomeric and dimeric Chl*a* in this medium. If the sample was excited at $\lambda = 710$ nm, EPR line shapes were observed that differed significantly from those obtained for $\lambda \leq 660$ nm.[32] A consistent interpretation of the triplet EPR spectra could only be achieved by exchanging the *X* and *Y* zero-field axes in the molecular frame between the two Chl*a* forms, that is, monomeric and dimeric (K. Laukenmann and G. Kothe, unpublished results).

4. Summary

In conclusion, we report high-frequency EPR data on the $P_{700}^{+\bullet}$ and P_{700}^T states in PS I in comparison with those of the Chl*a*$^{+\bullet}$ and Chl*a*^{T} states. These data present unambiguous proof that the electronic structures of the primary donor cation radical and triplet state are different from those of monomeric chlorophyll *a*. A dimeric structure of the primary donor and delocalization of the spin density in $P_{700}^{+\bullet}$ and P_{700}^T could account for these observations. The observed spectral effects cannot be accounted for simply by a strong interaction between P_{700} and the protein environment. Such an interaction cannot account for the larger shift of the g_z component compared to the g_x and g_y components in $P_{700}^{+\bullet}$ relative to Chl*a*$^{+\bullet}$. For the same reason, we rule out the proposed protein-interaction-induced mixing of the ground state with a closely lying excited state.[28] Future work will address the importance of environmental effects on the Chl*a*$^{+\bullet}$. As an alternative explanation for our observations, we suggest that trapping of the active species on the primary donor of PS I may occur because of the heteromeric character of P_{700}. Evidence that a reversible rearrangement of the geometric and electronic structure of Chl*a* can account for the observed differences in the magnetic resonance and redox properties between P_{700} and Chl*a* in vitro has been previously reported.[33] The authors proposed that an enolization of the ring V β-keto ester of Chl*a* is responsible for the change of the electronic properties of P_{700}. Additional confirmation of this hypothesis came recently from the X-ray crystal structure of PS I.[5] In this publication, a strong hydrogen bond with a keto group of ring V was reported for only one of the chlorophylls, Chl*a*′. Thus, Chl*a*′ might have at least a small admixture of the enol state. To resolve this question, we are attempting to record spectra of the Chl*a* enol cation radical and its triplet state by using high-frequency EPR.

A controversial issue for PS I is whether one or both branches of the electron-transfer pathways are active. The electronic structure of the P_{700} dimer is relevant to this question. Recent studies show that both branches are active, but the electron-transfer rates of the two branches are different.[34−36] These observations are easy to interpret in a dimer model. Delocalized excitation can facilitate electron transfer through one or another branch of the system. The difference in the electron-transfer rates might reflect asymmetry in the delocalization character of the unpaired spin density and triplet excitation. On the other hand, one may assume that bidirectional electron transfer is less likely within a heteromeric model of P_{700} in which one of the molecules is Chl*a* and another one is Chl*a*′-enol, with either one acting as a trap for the triplet state and the cation radical. A large difference in the redox properties of these two molecules would facilitate unidirectional electron transfer.

Acknowledgment. The authors express their appreciation to Prof. J. Norris and Prof. B. Barry for the fruitful discussions and useful comments regarding this work. Work was supported by the U.S. Department of Energy, Office of Basic Energy Sciences, Division of Chemical Sciences, under Contract W-31-109-Eng-38 (ANL) and Grant DE-FG02-01ER15281 (Yale).

References and Notes

(1) Snyder, S.; Thurnauer, M. C. In *The Photosynthetic Reaction Center*; Deisenhofer, J., Norris, J., Eds.; Academic Press: New York, 1993; p 285.

(2) Golbeck, J. H. In *Molecular Biology of Cyanobacteria*; Bryant, D. A., Ed.; Advances in Photosynthesis, Vol. 1; Kluwer Academic Publishers: Dordrecht, Netherlands, 1994; p 179.

(3) Norris, J. R.; Uphaus, R. A.; Crespi, H. L.; Katz, J. J. *Proc. Natl. Acad. Sci. U.S.A.* **1971**, *68*, 625.

(4) Emler, U.; Fritzsch, G.; Buchanan, S. K.; Michel, H. *Structure* **1994**, *2*, 925.

(5) Jordan, P.; Fromme, P.; Witt, H. T.; Klukas, O.; Saenger, W.; Krauss, N., *Nature* **2001**, *411*, 909.

(6) Feher, G.; Hoff, A. J.; Isaacson, R. A.; Ackerson, L. C. *Ann. N. Y. Acad. Sci.* **1975**, *244*, 239.

(7) Lubitz, W. In *Chlorophylls*; Scheer, H., Ed.; CRC Press: Boca Raton, FL, 1991; p 903.

(8) Artz, K.; Williams, J.; Allen, J.; Lendzian, F.; Rautter, J.; Lubitz, W. *Proc. Natl. Acad. Sci. U.S.A.* **1997**, *94*, 13582.

(9) Wasielewski, M. R.; Norris, J. R.; Crespi, H. L.; Harper, J. *J. Am. Chem. Soc.* **1981**, *103*, 7664.

(10) Käss, H.; Lubitz, W. *Chem. Phys. Lett.* **1996**, *251*, 193.

(11) Mac, M.; Bowlby, N. R.; Babcock, G. T.; McCracken, J. *J. Am. Chem. Soc.* **1998**, *120*, 13215.

(12) Breton, J.; Nabedryk, E.; Leibl, W. *Biochemistry* **1999**, *38* (36), 11585.

(13) Frank, H. A.; McLean, M. B.; Sauer, K. *Proc. Natl. Acad. Sci. U.S.A.* **1979**, *76*, 5124.

(14) Rutherford, A. W.; Setif, P. *Biochim. Biophys. Acta* **1990**, *1019*, 128.

(15) Budil, D. E.; Thurnauer, M. C. *Biochim. Biophys. Acta* **1991**, *1057*, 1.

(16) Sieckmann, I.; Brettel, K.; Bock, C.; van der Est, A.; Stehlik, D. *Biochemistry* **1993**, *32*, 4842.

(17) Krabben, L.; Schlodder, E.; Jordan, R.; Carbonera, D.; Giacometti, G.; Lee, H.; Webber, A. N.; Lubitz, W. *Biochemistry* **2000**, *39*, 13012.

(18) Käss, H.; Fromme, P.; Witt, H. T.; Lubitz, W. *J. Phys. Chem. B* **2001**, *105*, 1225.

(19) Prisner, T. F.; McDermott, A. E.; Un, S.; Norris, J. R.; Thurnauer, M. C.; Griffin, R. G. *Proc. Natl. Acad. Sci. U.S.A.* **1993**, *90*, 9485.

(20) Bratt, P. J.; Rohrer, M.; Krzystek, J.; Evans, M. C. W.; Brunel, L.-C.; Angerhofer, A. *J. Phys. Chem. B* **1997**, *101*, 9686.

(21) MacMillan, F.; Rohrer, M.; Krzystek, J.; Brunel, L.-C. In *Photosynthesis: Mechanisms and Effects*; Garab, G., Ed.; Kluwer Academic Publishers: Dordrecht, Netherlands, 1998; p 715.

(22) Bratt, P. J.; Poluektov, O. G.; Thurnauer, M. C.; Krzystek, J.; Brunel, L.-C.; Schrier, J.; Hsiao, Y.-W.; Zerner, M.; Angerhofer, A. *J. Phys. Chem. B* **2000**, *104*, 6973.

(23) Lakshmi, K. V.; Reifler, M. J.; Brudvig, G. W.; Poluektov, O. G.; Wagner, A. M.; Thurnauer, M. C. *J. Phys. Chem. B* **2000**, *104*, 10445.

(24) Goldman, S. A.; Bruno, G. V.; Polnaszek, C. F.; Freed, J. H. *J. Chem. Phys.* **1972**, *56*, 716.

(25) Grinberg, O. Y. High g-Resolution EPR Spectroscopy. Method and Applications. Thesis Dr. Science, Russian Academy of Sciences, 1988.

(26) Stewart, D. H.; Cua, A.; Chisholm, D. A.; Diner, B. A.; Bocian, D. F.; Brudvig, G. W. *Biochemistry* **1998**, *37*, 10040.

(27) Stone, A. *J. Mol. Phys.* **1963**, *6*, 509.

(28) O'Malley, P. J.; Babcock, G. T. *Proc. Natl. Acad. Sci. U.S.A.* **1984**, *81*, 1098.

(29) Link, G.; Berthold, T.; Bechtold, M.; Weidner, J.-U.; Ohmes, E.; Tang, J.; Poluektov, O. G.; Utschig, L.; Schlesselman, S. L.; Thurnauer, M. C.; Kothe, G. *J. Am. Chem. Soc.* **2001**, *123*, 4211.

(30) Zech, S. G.; Hofbauer, W.; Kamlowski, A.; Fromme, P.; Stehlik, D.; Lubitz, W.; Bittl, R. *J. Phys. Chem. B* **2001**, *104*, 9728.

(31) Vrieze, J.; Gast, P.; Hoff, A. J. *J. Phys. Chem.* **1996**, *100*, 9960.

(32) Münzenmaier, A.; Rösch, N.; Weber, S.; Feller, C.; Ohmes, E.; Kothe, G. *J. Phys. Chem.* **1992**, *96*, 10645.

(33) Wasielewski, M. R.; Norris, J. R.; Shipman, L. L.; Lin, C.-P.; Svec, W. A. *Proc. Natl. Acad. Sci. U.S.A.* **1981**, *78*, 2957.

(34) Hastings, G.; Sivakumar, V. *Biochemistry* **2001**, *40*, 3681.

(35) Guergova-Kuras, M.; Boudreaux, B.; Joliot, A.; Joliot, P.; Redding, K. *Proc. Natl. Acad. Sci. U.S.A.* **2001**, *98*, 4437.

(36) Muhiuddin, I. P.; Heathcote, P.; Carter, S.; Purton, S.; Rigby, S. E. J.; Evans, M. C. W. *FEBS Lett.* **2001**, *503*, 56.